GeoScienceWorld
Lithosphere
Volume 2024, Number 3, Article ID lithosphere_2023_322, 14 pages
https://doi.org/10.2113/2024/lithosphere_2023_322

Lithosphere

Research Article

Indirect Tensile Strength Test on Heterogeneous Rock Using Square Plate Sample with a Circular Hole

Xingzong Liu,[1] Bin Gong,[2] Kezhi Song,[1] and Hao Liu[3]

[1]*School of Civil Engineering, Ludong University, Yantai, China*
[2]*College of Engineering, Design and Physical Sciences, Brunel University London, London, UK*
[3]*Jinan Rail Transit Group Construction Investment Co., Ltd, Jinan, China*

Correspondence should be addressed to Bin Gong; bin.gong@brunel.ac.uk

Received 29 October 2023; Published 18 July 2024

Academic Editor: Enhedelihai Alex Nilot

An indirect testing method for determining the tensile strength of rock-like heterogeneous materials is proposed. The realistic failure process analysis method, which can consider material inhomogeneity, is applied to model the failure process of the square plate containing a circular hole under uniaxial compression. The influence of plate thickness and applied loads on the maximum tensile stress is investigated, and the tensile strength equation is deduced. Meanwhile, the initial cracking loads are obtained by the corresponding physical tests, and the tensile strengths are determined by substituting the initial cracking loads into the developed tensile strength equation. The values predicted by the newly proposed method are almost identical to those of the direct tensile tests. Furthermore, the proposed method can give the relatively small tensile strength error with the direct tensile test in comparison to the other test methods, which indicates that the proposed method is effective and valid for determining the tensile strength of rock-like heterogeneous materials.

1. Introduction

During the design process in geotechnical engineering, a crucial parameter is the tensile strength of rock [1, 2]. Direct tensile testing (DTT) is one of the most reliable methods for determining this strength and is independent of the constitutive response of a material [3, 4]. However, performing valid direct tensile tests is challenging. Preparing the dog bone-shaped specimens required for these tests is difficult, and stress concentrations at the ends of specimens often lead to failure away from the midpoint [5–7]. To use the direct methods, empirical equations from the literature are typically used, and/or numerous rock samples are tested in the laboratory. However, physical experiment is usually time-consuming and costly. Meanwhile, some indirect methods for assessing the tensile strength have been proposed [8–10]. The classical indirect testing methods include the ring test [11–13], wedge splitting test [14], three-point or four-point beam bending tests [15–17], hollow cylinder test [18], unconfined expansion test [19], point load test [20, 21], and Brazilian test [22, 23]. The Brazilian split test (BST) is the most commonly used indirect method to determine the tensile strength of rock-like materials, which is the recommended test method by the International Society for Rock Mechanics (ISRM) [24, 25]. However, the Brazilian test has been criticized since it was initially proposed due to the test results varying with loading rate [26–28], specimen size [29–31], experimental materials [32, 33], jaw's curvature [34], and testing standards [35]. In order to carry out a valid Brazilian test, researchers proposed plenty of modified Brazilian test methods [36–40].

Several factors control the tensile strength of rock materials, for example discontinuities, foliation, lamination, mineral composition, cementing material, hardness, and porosity [41–43]. Discontinuities, foliation, and lamination contribute to the heterogeneous structure of rock-like materials, which influences the macro-mechanical properties of rock-like materials [44–47]. They also greatly affect the disaster prevention and reduction in rock

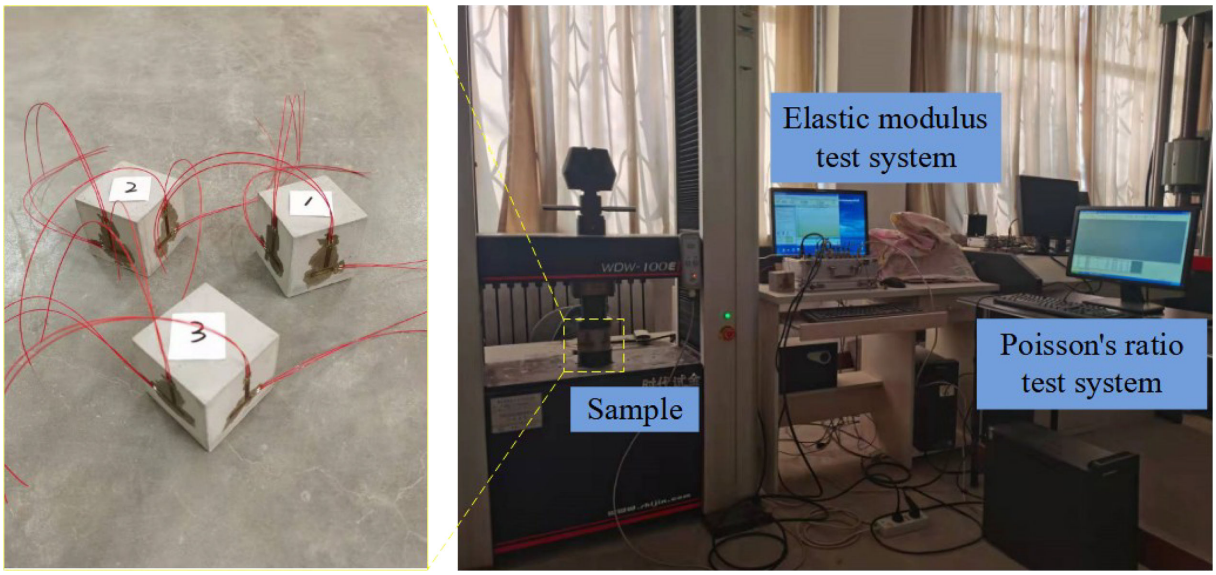

Figure 1: View of the sample for UCT.

engineering [48]. The formula of tensile strength under the assumption of isotropy was unreasonable [49]. Therefore, many researchers have studied the influence of rock anisotropy on tensile strength. For example, Roy and Singh [50] [50] studied the effect of the layer orientation on the tensile properties of granitic gneiss by using a Brazilian configuration and found that the layer orientation has a strong control over tensile strength. [51] addressed Brazilian tests on transversely isotropic rocks, experimentally and analytically, to identify failure conditions for a range of load contact types and anisotropy angles. Liu et al. [52] [52] analyzed the effect of bedding dip angle on the slate's tensile strength, failure modes, and acoustic emission characteristics. The above studies mainly focus on the anisotropy of rock structure. However, rock consists of a variety of mineral particles of different sizes, preexisting cracks, and the contacts between mineral particles, which contributes to the heterogeneity of rock. The heterogeneity of rock is difficult to be quantified in laboratory experiments [53, 54]. There are few methods to determine the tensile strength of rock-like materials by considering the heterogeneity.

In this study, a square plate model with a circular hole in the center was used to test the tensile strength of rock-like materials, and the heterogeneity of the material was considered during the testing process. First, the material heterogeneity was quantified by a uniaxial compression experiment and numerical simulation. Subsequently, the effect of model thickness and applied loads on the stress field is studied by the numerical simulation method considering material inhomogeneity. Furthermore, an indirect testing method considering material inhomogeneity to determine the tensile strength of rock-like materials is proposed. Finally, a physical experiment is carried out to verify the effectiveness of the method.

2. Quantification of the Material Heterogeneity

2.1. Numerical Expression of Material Heterogeneity. The realistic failure process analysis (RFPA) method has been widely used in rock mechanics [55–57]. The most important hypothesis reflected in the RFPA is that heterogeneity in rock strength causes progressive failure behavior. To simulate the random microstructures in rock, rock heterogeneity can be well characterized using statistical approaches [58–60]. Namely, a numerical model often consists of many meso-elements, and each element has its specific mechanical parameters. However, the statistical distribution of all the element mechanical parameters is assumed to obey the Weibull distribution function [61, 62], as detailed below:

$$\phi(f) = \frac{m}{f_0}\left(\frac{f}{f_0}\right)^{m-1} exp\left[-\left(\frac{f}{f_0}\right)\right]^{m-1}, \quad (1)$$

where m defines the shape of the Weibull distribution function, and it can be referred to as the homogeneity index, f is the mechanical parameters including the uniaxial compressive strength and elastic modulus, and f_0 is the mean value of the mechanical parameters of all elements. According to the Weibull distribution, the parameter m defines the shape of the density function, which defines the degree of material homogeneity. A larger m value indicates that more elements have mechanical properties that have been approximated to the mean value, which describes a more homogeneous rock specimen.

2.2. Uniaxial Compression Test of the Testing Material. A kind of engineering mortar passed through a sieve with a

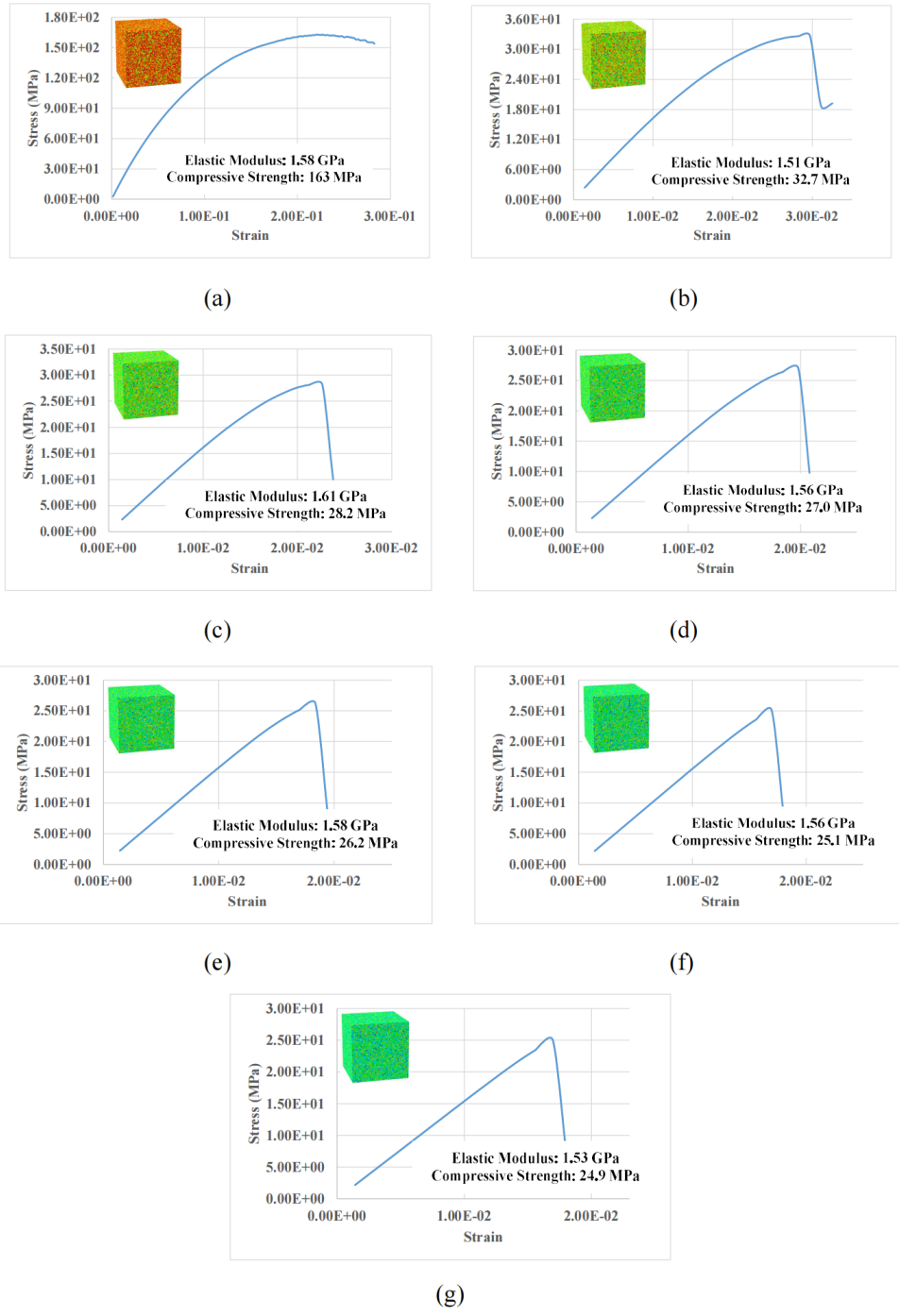

FIGURE 2: Numerical simulation results of UCTs with different homogeneity indices: (a) $m = 1$, (b) $m = 2$, (c) $m = 3$, (d) $m = 4$, (e) $m = 5$, (f) $m = 6$, and (g) $m = 7$.

diameter of 0.6 mm was used as the testing material in this study. The mortar and water were mixed in a ratio of 1:0.23. According to the Chinese standards (JGJ/*T* 70-2009), a cubic specimen with the dimensions of 70.7 mm × 70.7 mm × 70.7 mm was selected for the uniaxial compression test (UCT). Strain rosettes were glued on the lateral side of specimens, as illustrated in Figure 1.

As a result, the curves of stress–axial strain, as well as axial strain–lateral strain, can be obtained for each specimen. For each curve of stress–axial strain, the elastic modulus of the test mortar is determined as the slope of the stress–axial strain curve. The Poisson's ratio is the ratio of lateral strain to axial strain. The compressive strength is the peak of the stress–strain curve. UCTs were conducted by the way of displacement controlling using the WDW-100E mechanical testing machine with the maximum load of 100 kN. The loading rate applied by the test apparatus was set as 0.5 mm/min. As shown in Table 1, the elastic modulus of the experimental mortar used in this study was 1.53 GPa on average, whereas the compressive strength was 25.41 MPa

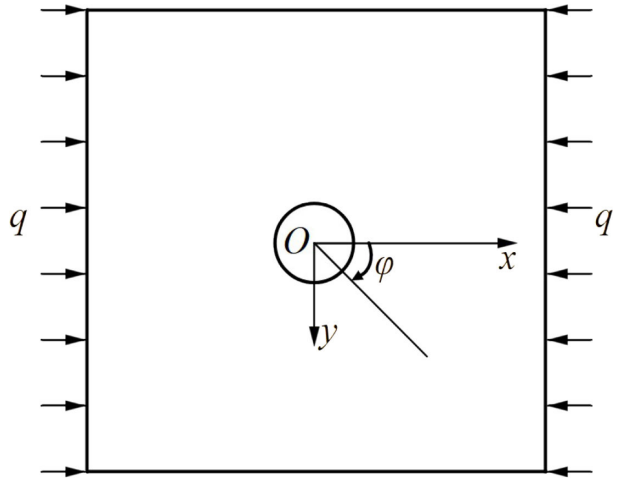

Figure 3: Model of a plate with a circular hole submitted to a symmetric uniform compression.

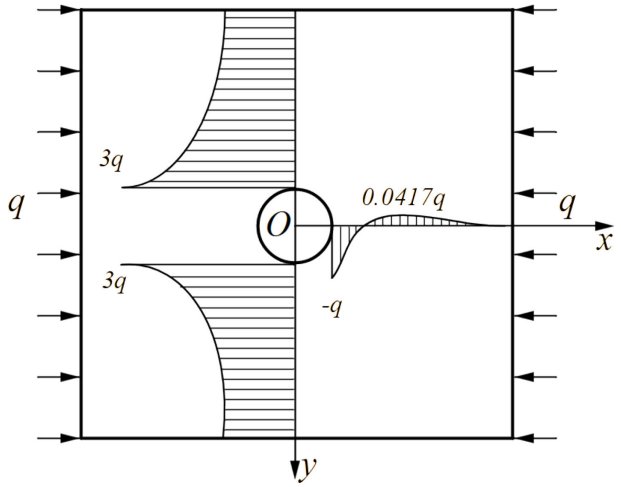

Figure 4: The distribution of σ_x along the y-axis and σ_y along the x-axis.

on average. The Poisson's ratio was reaching up to 0.33, averaging 0.30.

2.3. Determination of the Heterogeneity Index of the Testing Material. RFPA was used to build a three-dimensional (3D) numerical calculation model with the dimensions of 70.7 mm × 70.7 mm × 70.7 mm. The displacement loading was applied on the top of the model, and the bottom boundary of the numerical calculation model was fixed in the normal direction. The employed strength criterion was the Mohr–Coulomb failure criterion with a tension cutoff. This criterion governs the initiation of element damage, triggered when the stress state reaches the maximum tensile stress or Mohr–Coulomb thresholds. Initially, elements are assumed to exhibit linear elasticity, characterized by Young's modulus and Poisson's ratio. This linearly elastic behavior persists until the imposed stress exceeds the material capacity, at which point strain-softening occurs, altering the element response.

Table 1: Test results of UCTs for experimental mortar.

Sample number	Elastic modulus (GPa)	Compressive strength (MPa)	Poisson's ratio
1	1.58	24.58	0.27
2	1.50	25.96	0.30
3	1.50	25.70	0.33
Mean	1.53	25.41	0.30

To determine the heterogeneity index of the testing material, a series of numerical calculations were performed with the homogeneity index varying from 1 to 7 by referring to Tang [63, 64] . The properties of the numerical models were identical, and the physical and mechanical parameters used in the calculations were obtained through UCTs. The simulated results are summarized in Figure 2. As the homogeneity index m increases, the calculated elastic modulus fluctuates around the value measured by UCTs, while the compressive strength gradually decreases. When the homogeneity index m is 6, the calculated elastic modulus and compressive strength are closest to the values obtained from the tests. Therefore, it can be concluded that the homogeneity index of the testing material is 6.

3. A New Method to Determine the Tensile Strength of Rock-Like Heterogeneity Materials

3.1. Theoretical Basis. When the plate with a circular hole in the center is submitted to a symmetric uniform pressure of magnitude q in the x direction (Figure 3), the stress component at the edge of the hole in the cartesian coordinate system can be expressed by the following equation:

$$\begin{aligned}\sigma_x &= q(1-2\cos 2\varphi)\sin^2\varphi \\ \sigma_y &= q(1-2\cos 2\varphi)\cos^2\varphi \\ \tau_{xy} &= q(2\cos 2\varphi - 1)\sin\varphi\cos\varphi\end{aligned}, \tag{2}$$

where σ_x is the normal stress along the x-axis, σ_y is the normal stress along the y-axis, τ_{xy} is the shear stress in the xy plane, and φ is the included angle of a line rotated from the x-axis to a point. According to equation (2), the distribution characteristics of σ_x along the y-axis and σ_y along the x-axis are shown in Figure 4.

When the plate is submitted to a symmetric uniform pressure of magnitude q, the maximum compressive stress with $3q$ and the maximum tensile stress with $-q$ appear at the edge of the hole. The tensile strength of rock-like materials is much less than its compressive strength. When a rock-like plate with a circular hole in the middle of the plate is submitted to a symmetric uniform pressure, tensile failure will appear at the end of the hole near the loading surface, and the tensile stress at the time of failure is equal to the applied pressure.

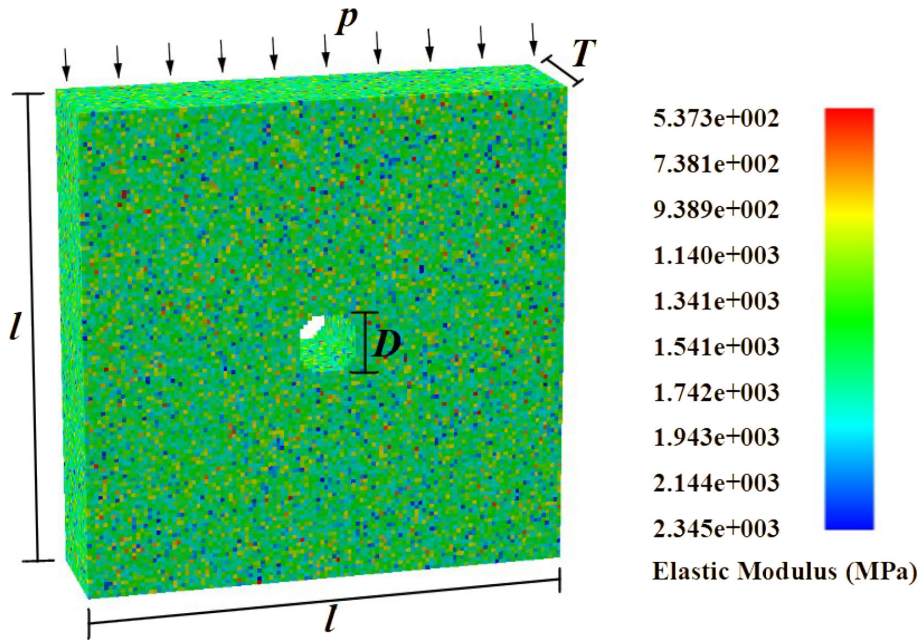

Figure 5: The 3D numerical calculation model.

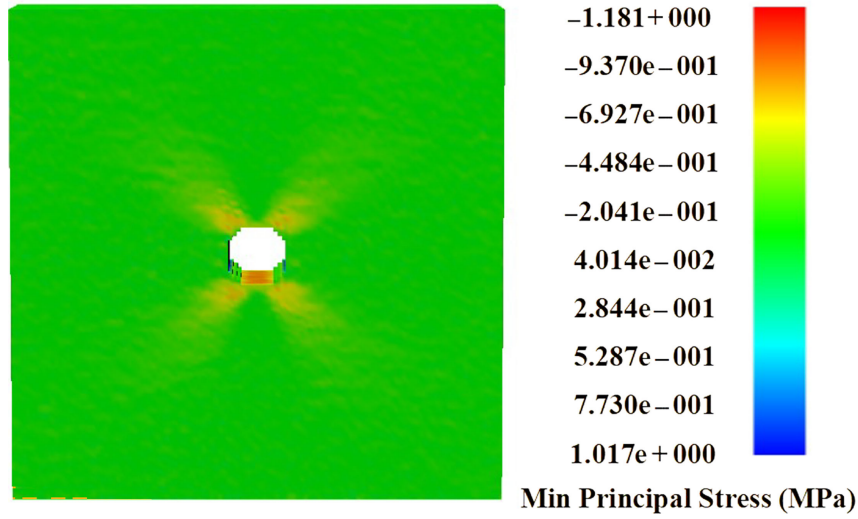

Figure 6: Minimum principal stress distribution of model (a negative value represents tensile stress).

3.2. Effect of Specimen Thickness on Tensile Stress Distribution. The theoretical analysis given in Section 3.1 is two dimensional (2D). The physical test model is 3D. Taking the use of 2D stress analysis to determine the tensile strength of a 3D model directly is unreasonable. In this section, a numerical calculation method was adopted to explore the variation rule of tensile stress distribution with the change of the plate thickness. RFPA was used to build a 3D model with length and height l = 24 cm and the diameter of the central circular hole D = 3 cm, as shown in Figure 5.

The ratio of thickness to diameter can be expressed as T/D with the thickness of the model is expressed by T. Uniform load P was applied on the top surface of the model. The bottom boundary of the numerical calculation model was fixed in the normal direction. To study the effect of specimen thickness on tensile stress distribution, a series of numerical calculations were performed with the T/D ratio varying from 0.1 to 2.0 and the uniform load P = 1 MPa. An elastic constitutive model was used, and mechanical parameters used in the calculation were presented in Table 1. The homogeneity index of numerical calculation material was 6. Considering the influence of material heterogeneity on the discretization of calculation results, five groups of parallel numerical calculations were carried out with the same homogeneity index in each working condition. A total of 100 numerical calculations were performed in this section.

Since the negative stress value in RFPA represents the tensile stress, the contour of minimum principal stress can be used to analyze the distribution law of the tensile stress

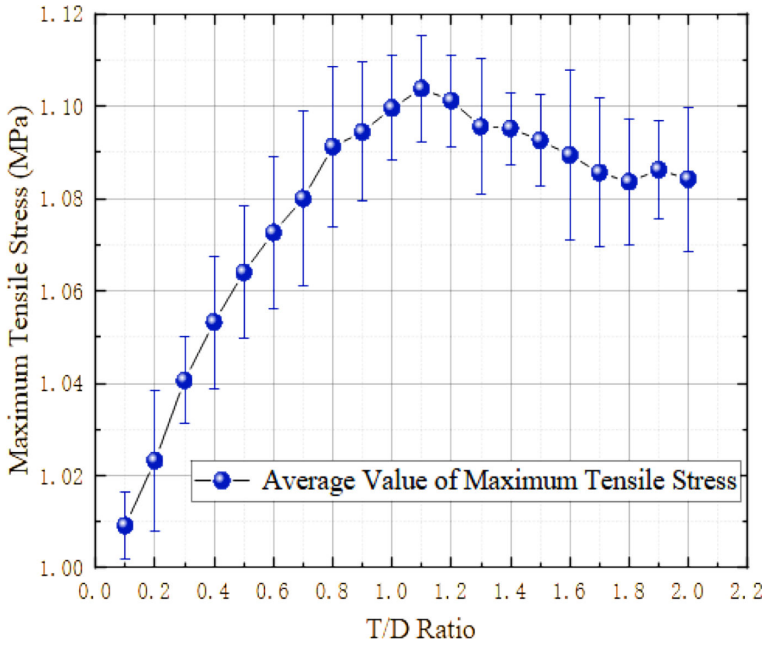

Figure 7: Maximum tensile stress of the model with the variation of model thickness.

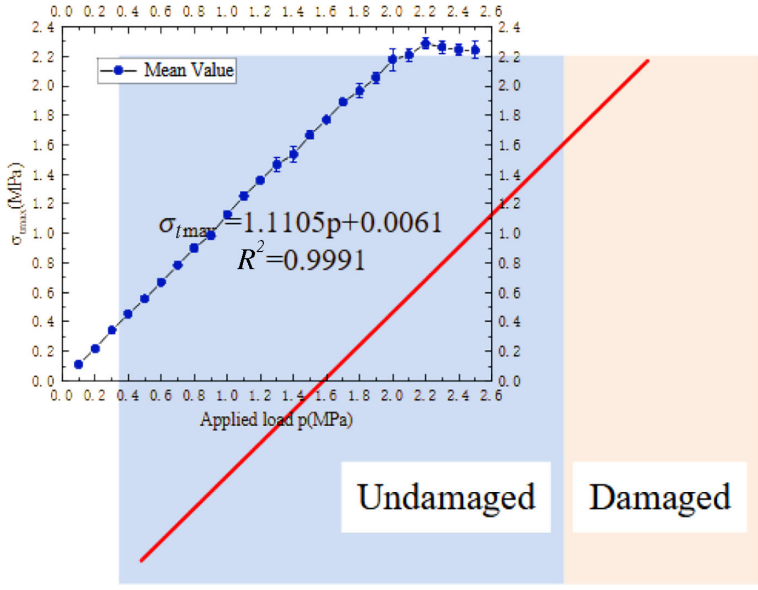

Figure 8: Relationship between the maximum tensile stress of the model and the applied load.

in the model. The distribution of the minimum principal stress of the model is shown in Figure 6. Due to the model failure first from the maximum tensile stress point, this section mainly focuses on the value and location of the tensile stress of the model. It is indicated by Figure 6 that the maximum tensile stress $\sigma_{t\max}$ occurs at the top and bottom of the hole, which is close to the loading surface. The maximum tensile stress of the model with the variation of model thickness is summarized in Figure 7.

When the T/D ratio and homogeneity index is constant, the randomness of material generation results in some fluctuations in the calculation results. The standard deviations are all less than 0.02, indicating that the discreteness of the calculated results caused by the randomness of materials is small. Therefore, the relationship between the maximum tensile stress and the T/D ratio can be analyzed by the average value of the calculated maximum tensile stress. As can be seen from Figure 7, the maximum tensile stress of the model first increases and then decreases as the thickness of the model increases. The peak of the maximum tensile stress appears when the T/D ratio of the model reaches a certain value. For the test material selected in this article, the peak of the curve occurs when the T/D ratio is equal to 1.1.

3.3. Effect of the Applied Load on Tensile Stress Distribution. Numerical calculations were also used to explore the determination method of the tensile strength of rock-like

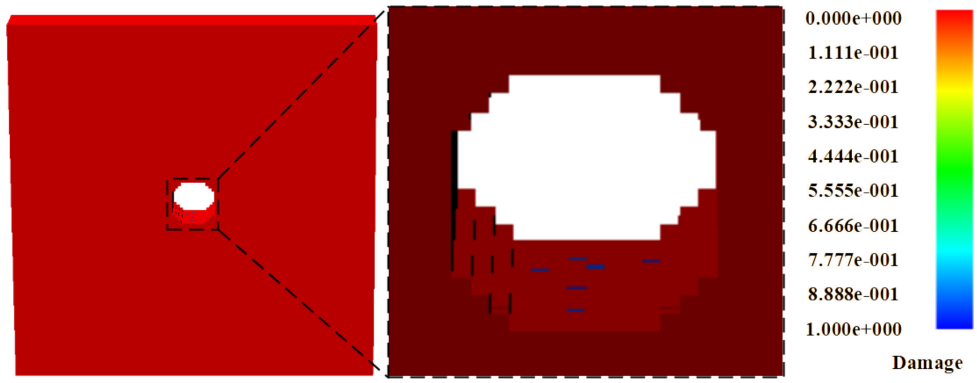

Figure 9: Distribution of damaged elements.

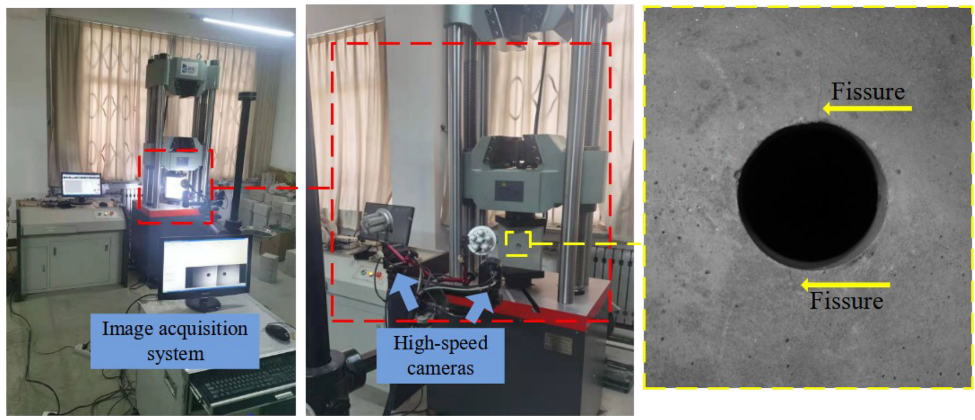

Figure 10: A real view of UCT combined with an image acquisition system.

heterogeneity materials. A series of numerical models were created with the T/D ratio is 1.1 and the applied load P varying from 0.1 to 2.5 MPa. The elastic–plastic constitutive model was used in this section. Assuming that the tensile strength of the material was one-tenth of the compressive strength, other material parameters used in the calculation were also presented in Table 1. The relationship between the maximum tensile stress of the model and the applied load is shown in Figure 8.

When the applied loads are small, the fluctuations of the calculation results caused by the randomness of the material are little, and the standard deviations are all less than 1%. When the applied load is large, the fluctuations of the calculated results become larger, but the standard deviations of the calculated results are all less than 10%. The discreteness of the calculated results caused by the randomness of materials is small. The relationship between the maximum tensile stress and the applied loads can be analyzed by the mean value of the calculated maximum tensile stress. When the applied load is less than 1.8 MPa, the maximum tensile stress has a linear relationship with the applied load. The linear fitting equation of maximum tensile stress and applied load can be expressed as follows:

$$\sigma_{\text{tmax}} = 1.1105p + 0.0061. \quad (3)$$

When the applied load exceeds 1.8 MPa, damaged elements appear at the top and bottom of the hole. In Figure 9, the serious damage occurring at the bottom of the hole is indicated by the blue elements. At this point, the maximum tensile stress of the model is greater than the tensile strength of the testing material, and the maximum tensile stress and the applied load no longer obey the linear relationship. Equation (3) is the relationship between the maximum tensile stress and applied loads when the model is in the elastic phase, which can be regarded as the tensile strength calculation formula. If the applied load at the beginning of the model failure can be obtained, the actual tensile strength of the material can be calculated by substituting the applied load at the beginning of the model failure into the tensile strength calculation formula. For the convenience of description, the new method proposed in this study is named the square plate test (SPT).

4. Comparison between the SPT and the Other Methods

In order to verify the validity of the new method proposed in this article, DTT, BST, three-point bending test (TPBT), and SPT were used to test the tensile strength of the engineering mortar mentioned earlier.

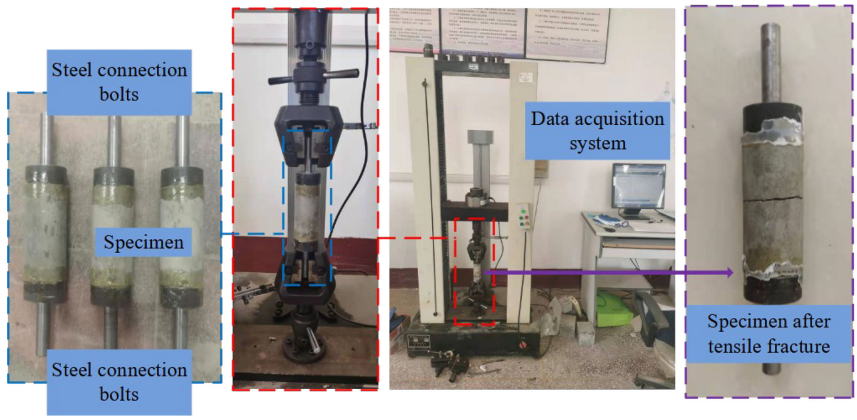

Figure 11: The specimens for direct tension tests.

(a) Specimens for Brazilian split tests

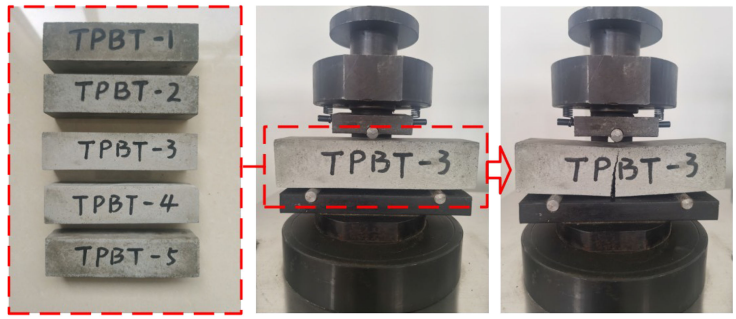

(b) Specimens for three-point bending tests

Figure 12: Specimens for (a) Brazilian split tests and (b) three-point bending tests.

Table 2: Test results of UCTs for plate samples.

Sample number	Initial cracking force (kN)	Initial cracking pressure (MPa)	Tensile strength (MPa)
1	21.56	2.72	3.03
2	21.76	2.75	3.06
3	21.94	2.77	3.08
4	22.24	2.81	3.13
5	22.58	2.85	3.17
Mean	22.02	2.78	3.09

Table 3: Results of direct tension tests.

Sample number	Peak load (kN)	Tensile strength (MPa)
1	4.97	2.99
2	5.30	3.19
3	5.40	3.25
Mean	5.22	3.14

4.1. Square Plate Test. The same engineering mortar mentioned earlier was used to establish the model shown in Figure 5, and the T/D was 1.1. The UCTs combined with an image acquisition system were performed to determine the loads of the specimen when the initial crack appeared. The loads were generated by the WAW-1000B mechanical testing machine with the maximum load of 1000 kN. The main component of the image acquisition system was two

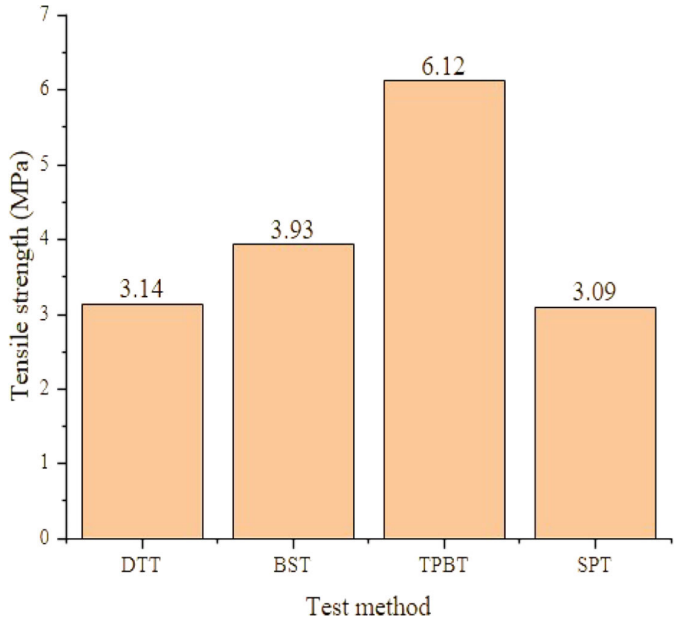

Figure 13: Average tensile strength from different test methods.

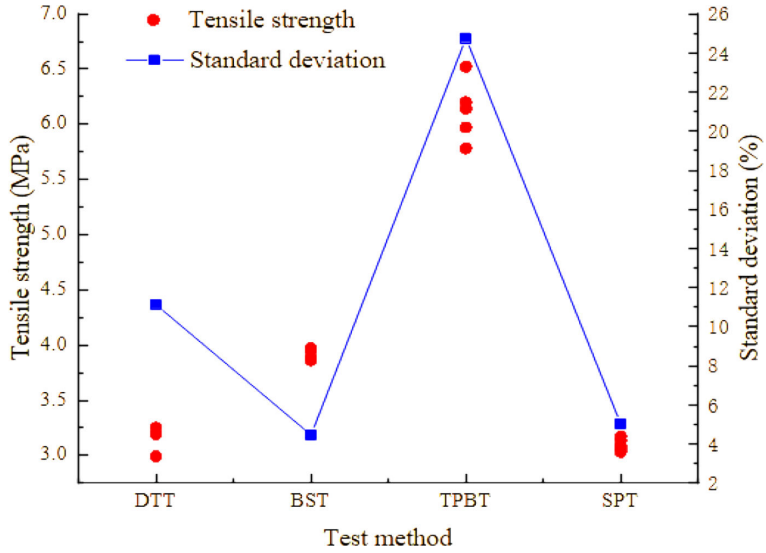

Figure 14: Measured tensile strength and standard deviation from different test methods.

Table 4: Results of Brazilian split tests.

Sample number	Peak load (kN)	Tensile strength (MPa)
BST-1	6.23	3.97
BST-2	6.06	3.86
BST-3	6.11	3.89
BST-4	6.22	3.96
BST-5	6.22	3.96
Mean	6.17	3.93

high-speed cameras. In order to better capture the initial crack load of the model, a strain gauge was attached to the inner surface of the circular hole close to the loading surface, and the applied load corresponding to the strain mutation was taken as the initial crack load of the model. A real view of UCT combined with the image acquisition system is shown in Figure 10.

The experimental results are listed in Table 2. The experimental results show that the initial cracking force is 22.02 kN on average, and the corresponding initial cracking pressure is 2.78 MPa on average. The tensile strength of the experimental mortar can be obtained by substituting the initial cracking pressure of 2.78 MPa into equation (3). After calculation, the tensile strength of the testing mortar is 3.09 MPa. The images captured by the high-speed camera (in Figure 10) show that the initial cracks appear at the top and bottom of the hole, which is consistent with the distribution of the damaged elements in the numerical

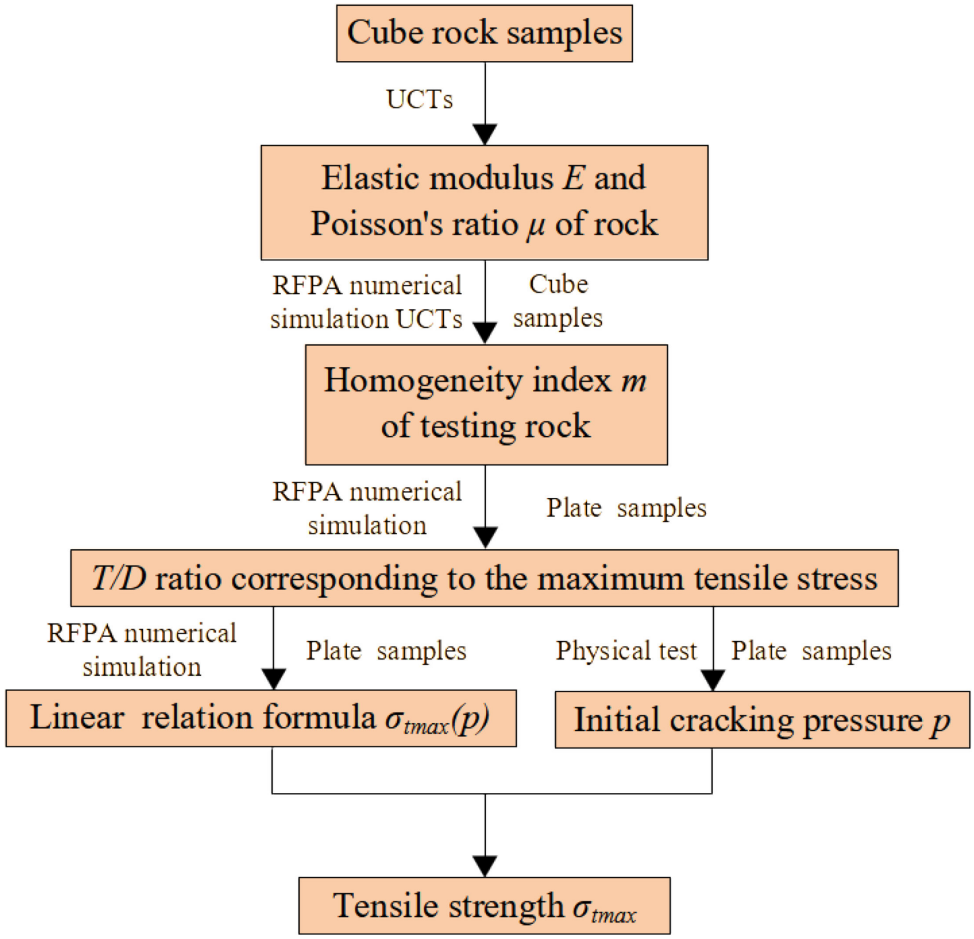

Figure 15: Implementing the new method to determine the tensile strength of rock-like heterogeneous materials.

simulation. The initiation and development of cracks begin in the region with the maximum tensile stress, which ensures the effectiveness of the new method for testing the tensile strength of materials.

4.2. Direct Tensile Testing. DTTs were carried out by using cylindrical specimens 46 mm in diameter and 100 mm in length to determine the tensile strength of the testing mortar. Two steel connection bolts were bonded on the top and bottom of the specimen, and the steel connection bolts were connected with the collets of the WDW-30 micro-computer-controlled electronic universal testing machine with the maximum load of 30 kN, as shown in Figure 11. The upper collet of the test machine was rotatable, which ensured the specimen was subjected to pure tensile stress. DTTs were carried out on the mortar cylindrical specimens. After the test, the failure section of the specimen was approximately horizontal, indicating that the specimen failed in the tensile model. The average tensile strength was 3.14 MPa, as shown in Table 3.

The SPT takes into account the heterogeneity of the material, and the tensile strength difference between the SPT and the DTT is less than 2%, which indicates that the SPT method is an effective method to test the tensile strength of rock-like heterogeneous materials. The testing method of tensile strength of materials mentioned in this study uses the regular shape of specimens, which can avoid eccentric compression or stress concentration in the loading process, and the test results have little dispersion. The principle of the SPT method is simple and easy to understand, which makes the SPT method proposed in this study expected to be widely used.

4.3. BST and TPBT. The BST is a recommended method to determine the tensile strength of rock-like materials by the ISRM and the American Society for Testing Material (ASTM). The tensile strength can be calculated using equation (4).

$$\sigma_t = \frac{2p}{\pi DT}, \tag{4}$$

where P is the applied load, D is the diameter of the disc, and T is the thickness of the disc. Taking into account the suggestions of the ISRM and the ASTM, the diameter of the Brazilian disc was 50 mm, and the thickness of the disc was 20 mm in this study (Figure 12(a)). The loading rate applied on the specimens was set as 0.5 mm/min. Another adopted testing method in this study was TPBT, in which the width

and height of the testing beam were all 40 mm, and the distance of the two bases was 100 mm (Figure 12(b)). BSTs and TPBTs are carried out by using the DYE-300 pressure testing machine with the maximum load of 10 kN.

The testing beam specimens were placed on two bases with a distance of 300 mm. The fracture will first occur at the bottom of the beam, and the corresponding tensile strength can be calculated:

$$\sigma_t = \frac{3pl}{2ba^2}, \tag{5}$$

where l is the distance of the two bases, b is the width of the beam, and a is the height of the beam. The results of the BSTs and TPBTs are listed in Tables 4 and 5, respectively. The average tensile strengths measured by BSTs and TPBTs are 3.93 and 6.12 MPa, respectively.

4.4. Test Results Comparison of BST, DTT, TPBT, and SPT. The average tensile strengths obtained by BST, DTT, TPBT, and SPT are summarized in Figure 13. The results of BSTs and TPBTs are greater than those of DTTs, and the results of SPTs are smaller than those of DTTs. The experimental results of TPBTs are about twice higher than those of the other tests, which is consistent with the findings of other researchers [15, 65, 66]. The absolute errors of the results of BST and TPBT with respect to DTT are 0.79 and 2.98 MPa, respectively. The relative errors of the results of BST and TPBT with respect to DTT are more than 25%. The absolute and relative errors of the result of SPT with respect to DTT are −0.05 MPa and 1.6%, respectively, indicating that the result of SPT is the closest to that of DTT.

Figure 14 reflects the measured tensile strength and standard deviation of different test methods. The standard deviation of the results of the BSTs and SPTs is less than 5%, indicating that the dispersion degree of the two test results is small, and the two methods can obtain the stable results. The DTTs and TPBTs have greater instability and less reproducibility, which is expected given by the complicated test setup, slight imperfections in specimens, and the test's low tolerance to sample imperfections. According to Figures 13 and 14, the SPT result is stable, and the result is consistent with those of DTTs. SPT can be considered to measure the tensile strength of rock-like heterogeneous materials. Figure 15 shows the flowchart to determine the tensile strength of rock-like heterogeneous materials.

Table 5: Results of three-point bending tests.

Sample number	Peak load (kN)	Tensile strength (MPa)
TPBT-1	2.55	5.97
TPBT-2	2.65	6.20
TPBT-3	2.78	6.52
TPBT-4	2.62	6.14
TPBT-5	2.47	5.78
Mean	2.61	6.12

5. Conclusions

In this study, based on the analytical solution of the elastic mechanics of a plate with a circular hole under symmetrical loads, the effect of model thickness and applied loads on the stress field is studied by the numerical simulation by considering material inhomogeneity. The main findings can be drawn as follows:

(1) The material heterogeneity can be quantified by a uniaxial compression experiment and numerical simulation. With the growth of applied loads, the damaged elements first appear in the region of the plate which possesses maximum tensile stress, and the failure mode is tension. Meanwhile, the maximum tensile stress of the model first increases and then decreases as the thickness of the model increases. The peak of the maximum tensile stress appears when the T/D ratio of the model reaches a certain value. Besides, the maximum tensile stress of the plate has a linear relationship with the applied load before the damaged elements appear in the plate.

(2) The SPT method to determine the tensile strength of rock-like heterogeneous materials can be summarized as follows: (a) the elastic modulus and Poisson's ratio of the material are measured by UCTs. Then, RFPA is used to simulate the uniaxial compression process under different homogeneity indices. The homogeneity index of the material is determined by comparing the numerical calculation results with the physical test results; (b) RFPA is used to establish the numerical model to study the influence of model thickness on the maximum tensile stress and to determine the T/D ratio corresponding to the maximum tensile stress of the testing material; (c) RFPA is used to establish the numerical model to study the influence of applied loads on the maximum tensile stress and to determine the linear relation formula between maximum tensile stress and applied loads; (d) the rock models are made and UCTs are carried out to obtain the initial crack load P; and (e) the tensile strength of the material can be calculated by substituting the load P obtained in step (d) into the linear relation formula obtained in step (c).

(3) The analysis process to determine the tensile strength of rock-like heterogeneous materials has been determined. The inhomogeneity of the material is considered in the new test method, and the results obtained by the new method are almost identical to those of the direct tensile tests, which indicates that the new method is effective to test the tensile strength of rock-like heterogeneous materials. The test specimen used in the new method has a regular shape which is easy to be prepared. The specimen

with an outer square and inner circle can effectively avoid the occurrence of eccentric compression or local failure of compression. Compared with the results of DTTs and TPBTs, the SPT results have less discreteness and better stability. Furthermore, SPT gave the smallest tensile strength difference with DTTs than the other test methods. The test equipment is simple, the principle is easy for understanding, the test results are stable, and the test results are consistent with those of DTTs, which improves the applicability of the proposed method. The limitation of this study is that only one material was tested. Actually, different types of rocks should be tested in further studies to provide more data for assessing the proposed test method.

Data Availability

The data underpinning this publication can be accessed from the Brunel University London's data repository, Brunelfigshare here under a CCBY licence: https://doi.org/10.17633/rd.brunel.25386487

Conflicts of Interest

The authors declare no conflict of interest.

Authors' Contributions

Xingzong Liu: investigation, formal analysis, data curation, visualization, funding acquisition, and writing—original draft; Bin Gong: conceptualization, methodology, supervision, and writing—review and editing; Kezhi Song: investigation and writing—review and editing; Hao Liu: formal analysis and visualization.

Funding Statement

This work was supported by the National Natural Science Foundation of China, China (grant no. 51978322).

References

[1] H. Fattahi and M. Hasanipanah, "An indirect measurement of rock tensile strength through optimized relevance vector regression models, a case study," *Environmental Earth Sciences*, vol. 80, no. 22, p. 748, 2021.

[2] Q. Ma, X. Liu, Y. Tan, et al., "Monitoring and evaluation of disaster risk caused by linkage failure and instability of residual coal pillar and rock strata in multi-coal seam mining," *Geohazard Mechanics*, vol. 1, no. 4, pp. 297–307, 2023.

[3] C. Z. Wu, X. G. Chen, Y. Hong, R. Q. Xu, and D. H. Yu, "Experimental investigation of the tensile behavior of rock with fully grouted bolts by the direct tensile test," *Rock Mechanics and Rock Engineering*, vol. 51, pp. 351–357, 2018.

[4] A. Fakhimi and J. F. Labuz, "A simple apparatus for tensile testing of rock," *International Journal of Rock Mechanics and Mining Sciences*, vol. 158, p. 105208, 2022.

[5] D. Y. Li and L. N. Y. Wong, "The Brazilian disc test for rock mechanics applications: Review and new insights," *Rock Mechanics and Rock Engineering*, vol. 46, pp. 269–287, 2013.

[6] Q. Y. Zhang, K. Duan, W. Xiang, S. B. Yuan, and Y. Y. Jiao, "Direct tensile test on brittle rocks with the newly developed centering apparatus," *Geotechnical Testing Journal*, vol. 41, no. 1, pp. 92–102, 2018.

[7] S. Demirdag, K. Tufekci, N. Sengun, T. Efe, and R. Altindag, "Determination of the direct tensile strength of granite rock by using a new dumbbell shape and its relationship with Brazilian tensile strength," IOP Conference Series: Earth and Environmental Science, vol. 221, p. 012094, 2019.

[8] A. Mahdiyar, D. J. Armaghani, A. Marto, M. Nilashi, and S. Ismail, "Rock tensile strength prediction using empirical and soft computing approaches," *Bulletin of Engineering Geology and the Environment*, vol. 78, no. 6, pp. 4519–4531, 2018.

[9] H. Harandizadeh, D. J. Armaghani, and E. T. Mohamad, "Development of fuzzy-GMDH model optimized by GSA to predict rock tensile strength based on experimental Datasets," *Neural Computing and Applications*, vol. 32, no. 17, pp. 14047–14067, 2020.

[10] H. Haeri, V. Sarfarazi, M. F. Marji, M. D. Yavari, and A. Z. Khameneh, "Direct tensile strength measurement of granite by the universal tensile testing machine," *Smart Structures and Systems*, vol. 27, no. 4, pp. 559–569, 2021.

[11] M. R. M. Aliha, P. Ebneabbasi, H. reza Karimi, and E. Nikbakht, "A novel test device for the direct measurement of tensile strength of rock using ring shape sample," *International Journal of Rock Mechanics and Mining Sciences*, vol. 139, p. 104649, 2021.

[12] Y. Zhang, S. Afroz, Q. D. Nguyen, et al., "Analytical model predicting the concrete tensile stress development in the restrained shrinkage ring test," *Construction and Building Materials*, vol. 307, p. 124930, 2021.

[13] B. H. Choi, Y. K. Lee, C. Park, C. H. Ryu, and C. Park, "Measurement of tensile strength of brittle rocks using a half ring shaped specimen," *Geosciences Journal*, vol. 23, no. 4, pp. 649–660, 2019.

[14] J. F. Guan, X. Z. Hu, C. P. Xie, Q. B. Li, and Z. M. Wu, "Wedge-splitting tests for tensile strength and fracture toughness of concrete," *Theoretical and Applied Fracture Mechanics*, vol. 93, pp. 263–275, 2018.

[15] Z. Y. Liao, J. B. Zhu, and C. A. Tang, "Numerical investigation of rock tensile strength determined by direct tension, Brazilian and three-point bending tests," *International Journal of Rock Mechanics and Mining Sciences*, vol. 115, pp. 21–32, 2019.

[16] V. P. Efimov, "Determination of tensile strength by the measured rock bending strength," *Journal of Mining Science*, vol. 47, no. 5, pp. 580–586, 2011.

[17] J. F. Guan, Y. L. Zhang, J. F. Meng, X. H. Yao, L. L. Li, and S. H. He, "A simple method for determining independent fracture toughness and tensile strength of rock," *International Journal of Rock Mechanics and Mining Sciences*, vol. 32, pp. 707–726, 2022.

[18] J. Z. Li, G. Zhang, and M. Z. Liu, "Experimental investigation on the effect of confining pressure on the tensile strength of

sandstone using hollow cylinder tensile test method," *Arabian Journal of Geosciences*, vol. 12, p. 768, 2019.

[19] Z. Tang, A. Tolooiyan, and R. Mackay, "Unconfined expansion test (UET) for measuring the tensile strength of organic soft rock," *Computers and Geotechnics*, vol. 82, pp. 54–66, 2017.

[20] M. Heidari, G. R. Khanlari, M. Torabi Kaveh, and S. Kargarian, "Predicting the Uniaxial compressive and tensile strengths of gypsum rock by point load testing," *Rock Mechanics and Rock Engineering*, vol. 45, no. 2, pp. 265–273, 2012.

[21] K. Karaman, A. Kesimal, and H. Ersoy, "A comparative assessment of indirect methods for estimating the Uniaxial compressive and tensile strength of rocks," *Arabian Journal of Geosciences*, vol. 8, no. 4, pp. 2393–2403, 2015.

[22] M. Mellor and I. Hawkes, "Measurement of tensile strength by diametral compression of discs and annuli," *Engineering Geology*, vol. 5, no. 3, pp. 173–225, 1971.

[23] N. Luo, H. Zhang, Y. Chai, et al, "Research on damage failure mechanism and dynamic mechanical behavior of layered shale with different angles under confining pressure," *Deep Underground Science and Engineering*, vol. 2, no. 4, pp. 337–345, 2023.

[24] A. Fahimifar and M. Malekpour, "Experimental and numerical analysis of indirect and direct tensile strength using fracture mechanics concepts," *Bulletin of Engineering Geology and the Environment*, vol. 71, no. 2, pp. 269–283, 2012.

[25] ISRM, "Suggested methods for determining tensile strength of rock materials," *International Journal of Rock Mechanics and Mining Sciences & Geomechanics Abstracts*, vol. 15, no. 3, pp. 99–103, 1978.

[26] X. H. Feng, B. Gong, X. F. Cheng, H. H. Zhang, and C. A. Tang, "Anisotropy and microcrack-induced failure precursor of shales under dynamic splitting," *Geomatics, Natural Hazards and Risk*, vol. 13, no. 1, pp. 2864–2889, 2022.

[27] X. Feng, B. Gong, Z. Liang, et al, "Study of the dynamic failure characteristics of anisotropic shales under impact Brazilian splitting," in *Rock Mechanics and Rock Engineering*, 57:pp. 2213–2230, 2024.

[28] D. Ji, H. Cheng, and H. Zhao, "Damage effect and progressive failure mechanism of sandstone considering different flaw angles under dynamic loading," *Rock Mechanics Bulletin*, vol. 3, no. 1, p. 100085, 2024.

[29] Y. Yu, J. Yin, and Z. Zhong, "Shape effects in the Brazilian tensile strength test and a 3D FEM correction," *International Journal of Rock Mechanics and Mining Sciences*, vol. 43, no. 4, pp. 623–627, 2006.

[30] Y. Yu, J. X. Zhang, and J. C. Zhang, "A modified Brazilian disk tension test," *International Journal of Rock Mechanics and Mining Sciences*, vol. 46, no. 2, pp. 421–425, 2009.

[31] P. Asadi, M. J. Ashrafi, and A. Fakhimi, "Physical and numerical evaluation of effect of specimen size on dynamic tensile strength of rock," *Computers and Geotechnics*, vol. 142, p. 104538, 2022.

[32] V. Sarfarazi, H. Haeri, P. Ebneabbasi, and K. Bagheri, "Simulation of the tensile behaviour of layered anisotropy rocks consisting internal notch," *Structural Engineering and Mechanics*, vol. 69, no. 1, pp. 51–67, 2019.

[33] J. Li, "Dynamic tensile mechanics and energy dissipation characteristics of sandstone under impact load," *China Mining Engineering*, vol. 52, no. 5, pp. 47–52, 2023.

[34] H. Yousefi and D. Fereidooni, "The effect of jaw's curvature on Brazilian tensile strength of rocks," *Geomechanics and Engineering*, vol. 23, no. 2, pp. 165–178, 2020.

[35] J. F. Liu, L. Chen, C. P. Wang, et al., "Characterizing the mechanical tensile behavior of Beishan granite with different experimental methods," *International Journal of Rock Mechanics and Mining Sciences*, vol. 69, no. 3, pp. 50–58, 2014.

[36] C. F. Markides, D. N. Pazis, and S. K. Kourkoulis, "The Brazilian disc under non-uniform distribution of radial pressure and friction," *International Journal of Rock Mechanics and Mining Sciences*, vol. 50, pp. 47–55, 2012.

[37] S. K. Kourkoulis, C. F. Markides, and P. E. Chatzistergos, "The standardized Brazilian disc test as a contact problem," *International Journal of Rock Mechanics and Mining Sciences*, vol. 57, pp. 132–141, 2013.

[38] E. Komurlu and A. Kesimal, "Evaluation of indirect tensile strength of rocks using different types of jaws," *Rock Mechanics and Rock Engineering*, vol. 48, no. 4, pp. 1723–1730, 2015.

[39] H. Lin, W. Xiong, and Q. X. Yan, "Modified formula for the tensile strength as obtained by the flattened Brazilian disk test," *Rock Mechanics and Rock Engineering*, vol. 49, no. 4, pp. 1579–1586, 2016.

[40] R. F. Yuan and B. T. Shen, "Numerical modelling of the contact condition of a Brazilian disk test and its influence on the tensile strength of rock," *International Journal of Rock Mechanics and Mining Sciences*, vol. 93, pp. 54–65, 2017.

[41] T. Efe, S. Demirdag, K. Tufekci, N. Sengun, and R. Altindag, "Estimating the direct tensile strength of rocks from indirect tests," *Arabian Journal of Geosciences*, vol. 14, no. 14, p. 143, 2021.

[42] G. Li, K. Wang, B. Gong, Z. Tao, K. Du, and C. Tang, "A multi-temporal series high-accuracy numerical manifold method for transient thermoelastic fracture problems," *International Journal of Solids and Structures*, vol. 230–231, 2021.

[43] Y. Wang, B. Gong, X. Yang, and C. Tang, "Investigation into the multistage mechanical damage behavior of columnar jointed basalts with different meso-constitutive relations and model sizes," *Lithosphere*, vol. 2023, no. 1, p. 8711959, 2023.

[44] Y. Wang, B. Gong, C. Tang, and X. Yang, "Size effect and lateral pressure effect on the mechanical resistance of columnar jointed basalt," *International Journal of Rock Mechanics and Mining Sciences*, vol. 171, p. 105571, 2023.

[45] X. Chen and Z. Qin, "A modified damage and fracture phase field model considering heterogeneity for rock-like materials," *Deep Underground Science and Engineering*, vol. 2, no. 3, pp. 286–294, 2023.

[46] C. Qi, C. Lu, A. I. Chanyshev, X. Li, and X. Qu, "Preliminary study on the determination of the Weibull modulus of strength distribution in quasi-brittle materials," *Geohazard Mechanics*, vol. 1, no. 2, pp. 103–109, 2023.

[47] O. Kolawole and F. Oppong, "Assessment of inherent heterogeneity effect on continuous mechanical properties of

shale via uniaxial compression and scratch test methods," *Rock Mechanics Bulletin*, vol. 2, no. 4, p. 100065, 2023.

[48] J. Xin, Q. Jiang, D. Zhai, G. Feng, B. He, and S. Li, "Shear-induced rockburst of double-tunnel rocks subjected to shear loading: a comparative analysis," *Journal of Central South University*, vol. 30, no. 12, pp. 4207–4229, 2023.

[49] J. Wei, J. R. Zhou, J. J. Song, Y. L. Chen, and P. H. S. W. Kulatilake, "Estimation of tensile strength and moduli of a tension-compression bi-modular rock," *Geomechanics and Engineering*, vol. 24, no. 4, pp. 349–358, 2021.

[50] D. G. Roy and T. N. Singh, "Effect of heat treatment and layer orientation on the tensile strength of a crystalline rock under Brazilian test condition," *Rock Mechanics and Rock Engineering*, vol. 49, pp. 1663–1677, 2016.

[51] Z. Aliabadian, G. F. Zhao, and A. R. Russell, "Failure, crack initiation and the tensile strength of transversely isotropic rock using the Brazilian test," *International Journal of Rock Mechanics and Mining Sciences*, vol. 122, p. 104073, 2019.

[52] P. Liu, Q. S. Liu, X. Huang, et al., "Direct tensile test and FDEM numerical study on nisotropic tensile strength of Kangding slate," *Rock Mechanics and Rock Engineering*, vol. 55, no. 12, pp. 7765–7789, 2022.

[53] R. H. Jiang, K. Duan, and Q. Y. Zhang, "Effect of heterogeneity in micro-structure and micro-strength on the discrepancies between direct and indirect tensile tests on brittle rock," *Rock Mechanics and Rock Engineering*, vol. 55, no. 2, pp. 981–1000, 2022.

[54] Y. Li and X. Wang, "Study on the dynamic characteristics of coal under different strain rates," *China Mining Engineering*, vol. 51, no. 4, pp. 93–97, 2022.

[55] T. T. Chen, G. R. Foulger, C. A. Tang, S. A. Mathias, and B. Gong, "Numerical investigation on origin and evolution of polygonal cracks on rock surfaces," *Engineering Geology*, vol. 311, p. 106913, 2022.

[56] Y. Y. Wang, B. Gong, and C. A. Tang, "Numerical investigation on anisotropy and shape effect of mechanical properties of columnar jointed basalts containing transverse joints," *Rock Mechanics and Rock Engineering*, vol. 55, no. 11, pp. 7191–7222, 2022.

[57] Y. Wang, B. Gong, Y. Zhang, X. Yang, and C. Tang, "Progressive fracture behavior and acoustic emission release of CJBs affected by joint distance ratio," *Mathematics*, vol. 10, no. 21, p. 4149, 2022.

[58] Y. Wang, B. Gong, C. Tang, and T. Zhao, "Numerical study on size effect and anisotropy of columnar jointed basalts under Uniaxial compression," *Bulletin of Engineering Geology and the Environment*, vol. 81, no. 1, p. 41, 2022.

[59] B. Gong, Z. Liang, and X. Liu, "Nonlinear deformation and failure characteristics of horseshoe-shaped tunnel under varying principal stress direction," *Arabian Journal of Geosciences*, vol. 15, no. 6, p. 475, 2022.

[60] C. Yu, B. Gong, N. Wu, P. Xu, and X. Bao, "Simulation of the fracturing process of inclusions embedded in rock matrix under compression," *Applied Sciences*, vol. 12, no. 16, p. 8041, 2022.

[61] B. Gong, T. Zhao, I. Thusyanthan, and C. Tang, "Modelling rock fracturing by a novel implicit continuous to discontinuous method," *Computers and Geotechnics*, vol. 166, p. 106035, 2024.

[62] M. Gao, B. Gong, Z. Liang, S. Jia, and J. Zou, "Investigation of the anisotropic mechanical response of layered shales," *Energy Science & Engineering*, vol. 11, no. 12, pp. 4737–4754, 2023.

[63] C. A. Tang, "Numerical simulation of progressive rock failure and associated seismicity," *International Journal of Rock Mechanics and Mining Sciences*, vol. 34, no. 2, pp. 249–261, 1997.

[64] Z. Z. Liang, C. A. Tang, H. X. Li, T. Xu, and Y. B. Zhang, "Numerical simulation of 3D failure process in heterogeneous rocks," *International Journal of Rock Mechanics and Mining Sciences*, vol. 41, pp. 323–328, 2004.

[65] L. Biolzi, S. Cattaneo, and G. Rosati, "Flexural/tensile strength ratio in rocklike materials," *Rock Mechanics and Rock Engineering*, vol. 34, no. 3, pp. 217–233, 2001.

[66] A. Coviello, R. Lagioia, and R. Nova, "On the measurement of the tensile strength of soft rocks," *Rock Mechanics and Rock Engineering*, vol. 38, no. 4, pp. 251–273, 2005.